INTERNATIONAL ATOMIC ENERGY AGENCY
UNITED NATIONS EDUCATIONAL, SCIENTIFIC AND CULTURAL ORGANIZATION

INTERNATIONAL CENTRE FOR THEORETICAL PHYSICS
34100 TRIESTE (ITALY) - P.O.B. 586 - MIRAMARE - STRADA COSTIERA 11 - TELEPHONE: 2240-1
CABLE: CENTRATOM - TELEX 460392 - I

SMR/302-60

COLLEGE ON NEUROPHYSICS:
"DEVELOPMENT AND ORGANIZATION OF THE BRAIN"
7 November - 2 December 1988

"Strange Attractors in Neural Networks"

Antonino BORSELLINO
SISSA
International School for Advanced Studies
Trieste, Italy

STRANGE ATTRACTORS
in
Neural Networks

A. BORSELLINO
ICTP and SISSA, Trieste

Ambiguous patterns are well studied in visual perception. The line drawings are interpreted as tridimensional "objects" in perspective and can be perceived with (at least) two different perspectives.

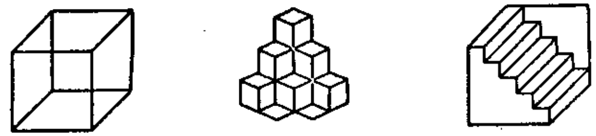

Necker cube Beehive Schroeder staircase

We studied the subsequent time intervals spent in the two "percepts", for example the lower square of the Necker cube as in front or in the back of the cube.

The statistical properties of the interval distribution are presented in Kybernetik, vol 10, pg 139-144 (1972).

The distribution is reproducible if the initial period of observation is discarded and the observer has been trained to "reverse". We suggest that he assumes an indifferent attitude, not favoring the reversal and not fighting it (a passive attitude).

By fitting the distribution of intervals with a "gamma" distribution, we characterize each observer with two parameters (n, b).

The two parameters are not "independent", see fig 5 in Kybern., pg 142.

The parameters for different patterns are "more or less" the same.

A similar experiment can be done putting the observer in acoustical ambiguity. He can hear the continuous repetition of two "phonemes" on a tape, like

--- pe - ra - pe - ra - pe - ra - pe - ra ----

$\underbrace{\text{pe - ra}}_{\text{pears (in ital)}}$ $\underbrace{\text{ra - pe}}_{\text{turnips}}$

and will shift from one meaning to the other. There is a strong correlation of the parameters of the reversal time of the auditory "channel" with those of the visual channel.

— A test of the parameters for the distributions of twin pairs has been studied, using the hospitality of the Institute for Genetics and Twins "G. Mendel" in Rome.

We observed 16 pairs of MZ twins and 16 pairs of DZ twins. The correlation between the parameters values of the real twins (monozygote) was very significative ($\rho_{1/2} = 0.79$) at the 0.05 level, while it was similar to the general population

for the dizygotic twins.

(see fig. 1 and 2 of the paper, in italian "Percezione... di gemelli monozigoti e dizigoti", Cybern. Congr. 1971 pg 204 - 207)

— We studied many other aspects of the reversal problems. For ex. how a stereoscopic cue (real) can stop or allow the reversal.

— One problem we have been confronted is due to the long time scale of the reversal: from seconds to ten seconds. Starting with real neurons, working at the time scale of ms we encountered difficulties in justifying the order of magnitude of $10^3 - 10^4$ times larger.

Using normal fluctuation of threshold, noise of synapses, etc we could just get a factor of $10 - 10^2$. There is a discrepancy of the order of the factor 10^2.

We used the ordinary "statistical" approach of coarse grain approximation as proposed by Harth or Cowan - Wilson.

Furthermore we would like to obtain the statistical properties of the phenomenon (the gamma distribution)

Mightly from the model, without "coup de pouce".

For this reason we welcomed the new dynamics for non linear systems of sufficient high dimensions (at least 3), showing that such systems can show "strange attractors", with two basin of attraction, like the Lorenz system, the first discovered in a problem of meteorology.

We thought we could justify the long time duration as a "dwindling" time, spent spiralling inside one basin and the reversal as a transition to the other basin.

We performed an analysis of such a game for the known strange attractor (See: Biol. Cyb. 55, 377-385, 1987) and the result are encouraging.

We tested also the neuronal models studied by Cowan and Ermentrout (1984)

$$\begin{cases} \dfrac{dE}{dt} = -\rho E + a_{13} S_1(P) \\ \dfrac{dI}{dt} = -KI + a_{12} S_1(P) \\ \dfrac{dP}{dt} = -P + a_{11} S_1(P) + a_{21} S(I) + a S_{31}(E) \end{cases}$$

with 3 groups of neurons: Excitatory (E), Inhibitory (I) and "Pyramidal cells" (P); $S(X)$ and $S_1(X)$ are

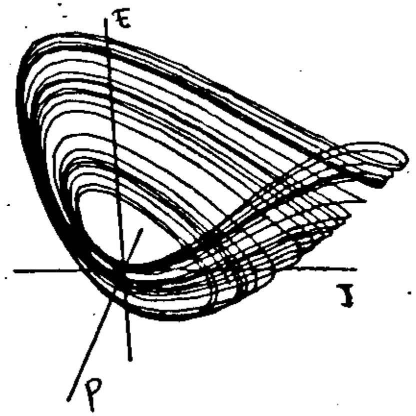

G.B. Ermentrout and J.D. Cowan (1979)
Temporal oscillations in neuronal nets
J. Math. Biol, 7., pp 265-280

G.B. Ermentrout (1984)
Period doublings and Possible chaos in neuronal models
Siam J. Appl. Math, Vol 44, No 1 pp 80-95

logistic functions, expressing the synaptic connections between the different types of cells.

C & E shows that the systems can present a strange attractor, but only with a single basin of attraction.

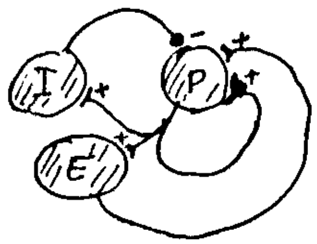

We studied another possible network, again with 3 groups, with the more general equations:

$$\begin{cases} \dfrac{dx}{dt} = ax + b_1 y + dzy \\ \dfrac{dy}{dt} = ay + b_2 x + exz \\ \dfrac{dz}{dt} = cz + fxy + g \end{cases}$$

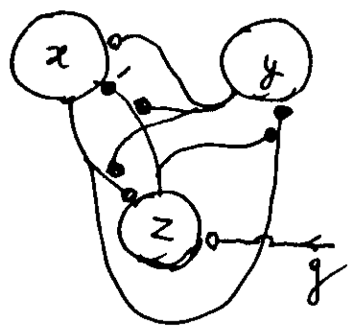

The non linearity is obtained via an axo-axonic modulation (products zy, xz, xy).

Choosing the values:

$a = -1$ $\quad d = -0.4$
$b_1 = 1$ $\quad e = -0.4$
$b_2 = 1$ $\quad f = 1$
$c = .01$ $\quad g = 1$ (with the meaning of external stimulation).

The strange attractor presents now two basins and the alternance between the two basins follows quite well the gamma-distribution, with a mean time of permanence of the order of seconds.

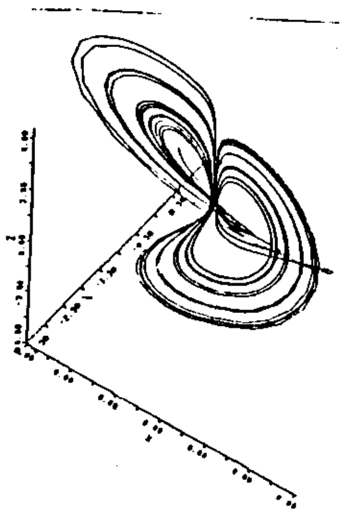

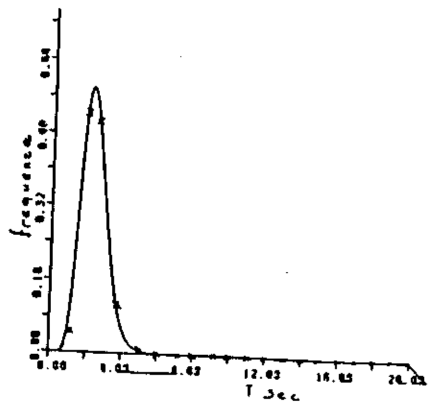

– Another approach we are exploring is in the philosophy of the parallel distributed processing (PDP). One possibility is to describe the Necker cube giving to each vertex a "neuron" to work with, with constraints (excitatory or inhibitory) from the other neurons.

See Rumelhart, Smolensky, McClelland and Hinton, Chapter 14 (2nd vol) of the PDP Bible.

The goodness-of-fit surface has two opposite peaks, but they are fixed points (stable). We are exploring how to convert this static description in a dynamical one.

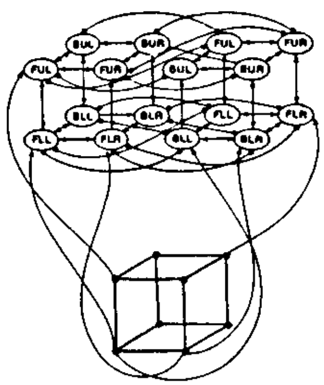

FIGURE 1. A simple network representing some of the constraints involved in perceiving the Necker cube.

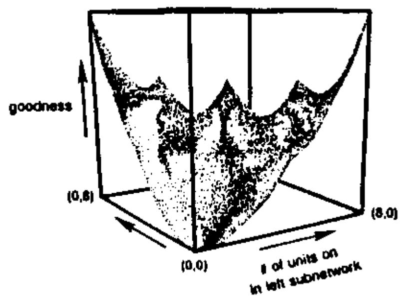

FIGURE 3. The goodness-of-fit surface for the Necker-cube network. The low point at the (0,0) corner corresponds to the start state. The peaks on the right and left correspond to the standard interpretations of the Necker cube, and the peak in the center corresponds to the impossible Necker cube illustrated in the previous figure.

$$a_j(t+1) = a_j(t) + \begin{cases} net_j(1 - a_j(t)) & net_j > 0 \\ net_j a_j(t) & \text{otherwise.} \end{cases}$$

Kybernetik 10, 139–144 (1972)

Reversal Time Distribution in the Perception of Visual Ambiguous Stimuli

A. Borsellino, A. De Marco, A. Allazetta, S. Rinesi, and B. Bartolini

Laboratorio di Cibernetica e Biofisica del CNR, Camogli, Istituto di Scienze Fisiche dell'Università di Genova, and Istituto di Fisica Generale dell'Università di Torino, Italy

Received August 4, 1971

Abstract. Reversal of perspective for ambiguous optical stimuli (Necker cube, Schröder staircase, honeycomb) has been studied, determining the statistical distribution of time intervals spent on each percept. The experimental distributions can be fitted with the gamma function, characterized by two parameters α, b. The two parameters are not independent, showing a correlation $\varrho = 0.74$.

Subsequent intervals appear to be largely independent; from the beta distribution for the fraction of time spent on a given percept, one can show that the subjects differ only in regard to the variance of this variable.

1. Introduction

Ambiguous perceptual stimuli are those able to elicit different perceptions. A very notable fact is that these perceptions alternate during continued observations of the same stimulus, giving us the possibility of registering the subsequent intervals of time for each perception and thereby obtaining information about properties of the neural machinery involved in the processing of the stimulus.

A well known class of ambiguous stimuli are visual forms eliciting perception of solid bodies as seen in two different perspectives. The oldest known is the Necker cube (1832), but many others were later discovered; the Mach book, the Schröder staircase, the honeycomb. Another well known category is given by those visual forms generating the figure-ground alternations.

Interest in the field of visual ambiguous stimuli has varied in the past. What has been often unusually distressing is the very large variability involved, depending on choice of subjects, their experimental conditioning, choice of the visual stimulus, dependence on its size, brightness, complexity, etc. All this high variability has caused the disappointing result that, notwithstanding a century of extensive research, not a single quantitative law has been derived from the experiments.

However Frederiksen *et al.* (1934) noted the high reproducibility of the measurements of the reversal rate for the Necker cube in 95 Ss, found ranging from 4.6 to 74.4 per minute, expressed the opinion that "a test with such high reliability and such a wide range of measurements must be a delicate indicator of some constant factor or set of factors in the individual". The same opinion was expressed as late as in 1969 by Künnapas at the conclusion of an unsuccessful search for a "personal tempo, to be correlated to the reversal rate of figural fluctuations".

Due to the high level of neural mechanism, certainly behind the optical chiasma (Cohen, 1959; Brown, 1962), responsible for the perceptual alternation with visual patterns and to the simple procedure to get "reliable" data, we thought it was worthwhile to make a more sophisticated approach at the individual level, with the aim to describe the individual variability. This approach started (Borsellino, 1967) with the attempt to separate a pattern ambiguity, as expressed by an informational entropy H, from the additional incertitude due to the statistical distribution of intervals, that could possibly be considered as an individual characteristic of the observer.

We report here the results obtained for the interval distribution, as a useful tool in describing the observer's behavior.

2. Procedure

The S is sitting at a table, looking binocularly at a screen at 2 m distance, on which the ambiguous visual form is projected, in size 40×40 cm², from

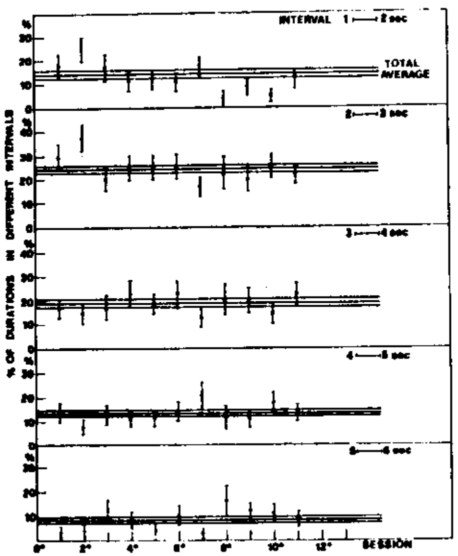

Fig. 1. Percentages of duration for one perception of the Necker cube (cube down), in 11 sessions for the same subject. The relative frequencies are given separately for intervals ranging from 1–2 to 5–6 sec. The vertical segments represent the statistical errors of each session

slides. The room is dimly illuminated and the S is told to fixate the center of the drawing, without any effort to keep one of them or to favour the reversals. At each reversal the S moves horizontally the index finger of his right hand, cutting small beams of light impinging on phototransistors. With this minimal effort, the S sends signals to a paper recorder (Sanborn) and to a magnetic tape recorder. The paper tracings are used for direct control in the course of the experiments and the magnetic tapes are used for subsequent computer analysis.

3. Analysis of Data

In the cases of figure-ground alternations (Künnapas, 1969) it has been shown that, as for movement alternations (Brown, 1953, 1955), the rate of alternations increases regularly during the first 2–3 min of observations. After this initial phase, the rate reaches a value that remains constant within statistical fluctuations.

Our Ss were tested using as reversible perspectives the Necker cube or the Schröder staircase and we found in general the same increase of the reversal rate after 2–3 min of continued fixation.

Since we are interested in the more stable phase, all our data that will be reported here, refers to this "stationary" behavior, i.e. after the transient or initial phase is finished.

For each S the intervals t_i appear to be spread widely around the mean value $\bar{t}$. For 10 Ss we repeated the test in different hours and days, to get indications concerning the reproducibility of the distribution of intervals.

We give in Fig. 1 the results obtained for one subject (B.C.). In this case we measured, for the Necker cube, the durations of one of the two perceptions, collecting not less than one hundred values, and this was repeated for 11 sessions. The percentages of durations taken in each session are presented separately, for interval durations in the ranges 1–2 sec, 2–3 sec, 4–5 sec, 5–6 sec. One can see how the sampled percentages fluctuate around the total averages. We represented with a vertical segment the amplitude of the fluctuation in the percentages, for the subsequent sessions, $K = 1, 2, \ldots, 11$, as expected on purely statistical grounds. On the same diagrams we reported also the fluctuation for the total distribution, and one can see that very few points lie away from the general mean by more than one sampled σ_K.

Analogous results obtained for all these Ss indicate that the high reliability already noted by Frederiksen *et al.* (1934) for the mean rate can be considered valid also for the distribution of intervals.

4. Distributions and Their Representation

The distribution of the intervals for one perception in all our Ss has been found to be unimodal, asymmetric, with a more or less fast growth and a long tail. We given in Fig. 2 the distribution obtained for the previously (Fig. 1) discussed subject B.C.

The experimental points are shown in the diagram, together with their statistical errors (vertical bars). Our next aim has been to get an analytical representation of the results, using some simple theoretical distribution.

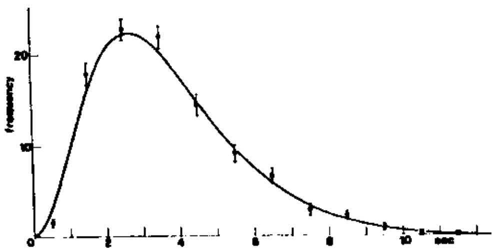

Fig. 2. Distribution of the duration of one perception of the Necker cube (cube down) for the subject B.C. with a sample of 1100 measurements. The full line is the theoretical distribution (1) (see text) with $n = 4.3$ and $b = 0.9$ sec^{-1}

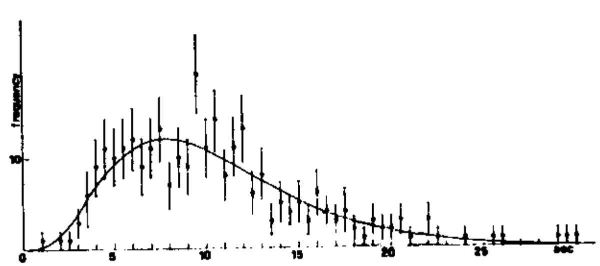

Fig. 3

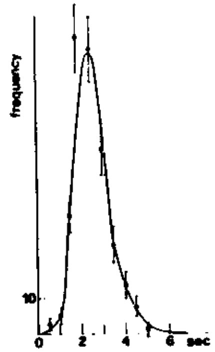

Fig. 4

Fig. 3. Distribution of the durations of one perception of the Necker cube (cube down) for a "slow" subject (A.G.); the full line is the theoretical distribution (1) with $n = 4.3$ and $b = 0.4$ sec^{-1}

Fig. 4. Distribution of the durations of one perception for the Necker cube (cube down) for a "fast" subject (A.C.). The full line is the theoretical distribution (1) with $n = 9$ and $b = 3.9$ sec^{-1}

One possible distribution, with the general properties indicated by the experimental results, is the χ^2 distribution. This is a one parameter distribution (degrees of freedom m) and, applying the method of moments, we tried it on our points, taking $\chi^2 = (t/\bar{t})^2$. We had to discard it, because the best fit gave a result much below the 1% level.

We tried than the 2-parameters gamma distribution:

$$\Gamma(t) = \frac{(bt)^n e^{-bt}}{t\,\Gamma(n)}, \quad \Gamma(n) = (n-1)! \tag{1}$$

where b and n are two free parameters. Using the same method of moments, based on the relations:

$$b = \frac{\bar{t}}{\sigma_t^2}, \quad n = \frac{\bar{t}^2}{\sigma_t^2} \tag{2}$$

where $\bar{t}$ is the average and σ_t^2 is the variance, the curve fitting is satisfactory. In Fig. 2 we show the curve with $b = 0.9$ sec^{-1} and $n = 3.4$, to be compared with the experimental data previously discussed.

If we apply the maximum likelihood criterion, computationally more laborious, we get results not very different.

5. Exactness of Fit for Subject's Population

Our procedure was applied on 24 Ss chosen from among our colleagues or from volunteering or hired science students. In all cases we found that the distributions were such that a "fast" subject could be called also "regular" while a "slow" subject would also be called "irregular". Two extreme cases are shown in Figs. 3 and 4. The same two different types of Ss were already found by Washburn *et al.* (1931).

All our Ss were tested on 3 ambiguous stimuli, the Necker cube, the Schröder staircase and the honeycomb. For each stimulus we obtained the distribution of intervals separately for each of the two possible perceptions.

For 24 of these Ss we computed the χ_0^2, to express the exactness of the fitting of the theoretical curve (Γ) on the experimental points. Out of the $144 = 24 \times 3 \times 2$ distributions, we found 43 of them for which the probability $P(\chi^2 > \chi_0^2)$ was less than 1% so they would be discarded.

It is well known that in some few cases the S gets blocked or gets in troubles in signaling correctly. We thought that we could possibly keep under control this type of "inconvenience", by discarding all intervals for which we would have $t > \bar{t} + 3\sigma_t$. Accepting this quite arbitrary criterion, we computed again all the Γ distributions, their χ_0^2 and we found that only in 24 cases out of 144 did we get $P(\chi^2 > \chi_0^2) < 0.01$.

In what we refer now about properties of our population of Ss, all the theoretical curves and the determination of the two parameters n, b are obtained with the above said computational rule, i.e. disregarding all the measured intervals $t > \bar{t} + 3\sigma_t$.

Naturally we are aware that we cannot give a justification for the above procedure. But in the present situation we consider it satisfactory to be able to use the same distribution function for our Ss, within the confidence level for 85% of them.

We tried also other possible two parameters distribution functions, e.g. the Wiener distribution for random walk with drift with one absorbing barrier. Due to the faster rising and slower descent of this distribution, the fit resulted worse.

6. Correlation between n, b

With the statistical rules previously described, we expected that all the variability of the Ss behavior, in the ambiguous perceptual situation of the experiment, would be taken into account by the distribution of intervals as fixed by the two parameters n, b. Our next step was therefore to see how the value of the parameters would be distributed and we plotted the scatter diagram, in which a point (b, n) corresponds to a S.

The result is shown in Fig. 5, for the Necker cube. We have taken for n and b the mean value of the

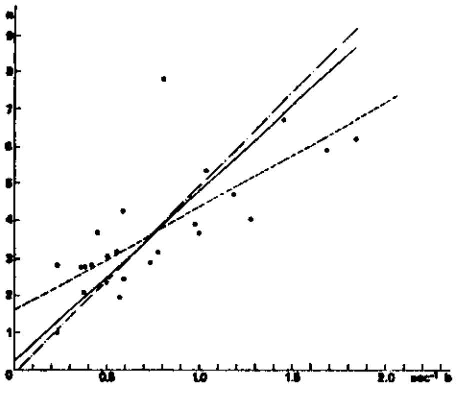

Fig. 5. Scatter diagram n vs. b for the Necker cube for 24 Ss. The correlation coefficient is $\varrho = 0.74$ and the best regression line (full line) is

$$n = 4.6\, b + 0.2$$

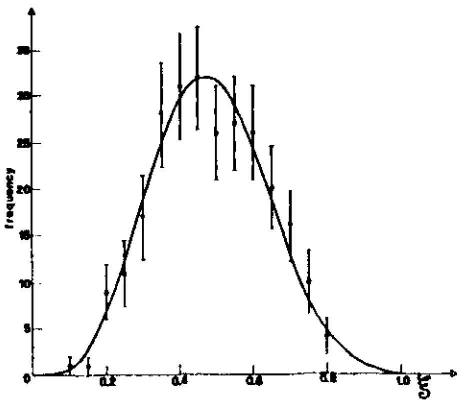

Fig. 6. Distribution of the elementary probability relative to the subject A.A. The full line is the theoretical distribution (8) with $p = 5.45$ and $q = 4.55$

respective values of the two perceptions which are practically equal.

The two parameters are not independent and we obtain a correlation coefficient $\varrho = 0.74$.

We have calculated 3 regression lines; the first one (dashed line) supposing b as independent variable, the second (dotted line) supposing n as independent variable and the last (full line) with the methode of orthogonal projections. The linear relationships obtained are, respectively:

$$n = 1.6 + 2.7\, b$$
$$n = -0.1 + 4.9\, b$$
$$n = 0.2 + 4.6\, b\,.$$

We must admit that this quite strong correlation was unexpected in view of the difficulty of fitting the interval distributions with a single parameter curve. In fact, we need both parameters to get a satisfactory fit for each S at the assigned confidence level. So the second degree of freedom is necessary, but the above result indicates that, once the first parameter is determined, the chances are high that we will pick a partially determinate value for the other one.

7. Interval Independence and Equivalence to β Distribution

Our data have also been submitted to a further analysis to find out if the duration of a perception keeps in some way the memory of the duration of the prior one.

We have so calculated the correlation coefficient between two successive perceptions and we have found for it a value around 0.19.

We can so conclude that in the transition from one perception to another, about all the memory of the duration of the prior perception has been destroyed.

This important fact permits us to display our data in another way: let be t_1 the stochastic variable relative

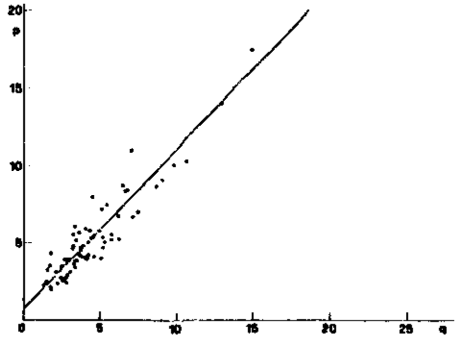

Fig. 7. Scatter diagram of parameters p and q of the distribution (8). The correlation coefficient is $\varrho = 0.93$ and the best regression line is $p = 1.0\, q + 0.7$

to the duration of the perception "cube down" and t_2 that relative to the "cube up".

If the distribution of t_1 and t_2 follows (1), with parameters n_1, b_1 and n_2, b_2 respectively, it is possible to show that the stochastic variable

$$\xi = \frac{t_1}{t_1 + t_2} \qquad (5)$$

follows a distribution with a density

$$f(\xi) = \frac{\Gamma(n_1 + n_2)}{\Gamma(n_1)\,\Gamma(n_2)}\, b_1^{n_1} b_2^{n_2} \frac{\xi^{n_1-1}(1-\xi)^{n_2-1}}{[(1-\xi)\, b_2 + \xi\, b_1]^{n_1+n_2}}\,. \qquad (6)$$

Now if $n_1 = n_2 = n$ and $b_1 = b_2 = b$, that is if the two perceptions have the same distribution, than (6) becomes

$$\beta(\xi) = \frac{\Gamma(2n)}{\Gamma^2(n)}\, \xi^{n-1}(1-\xi)^{n-1} \qquad (7)$$

that is a β distribution with only one parameter

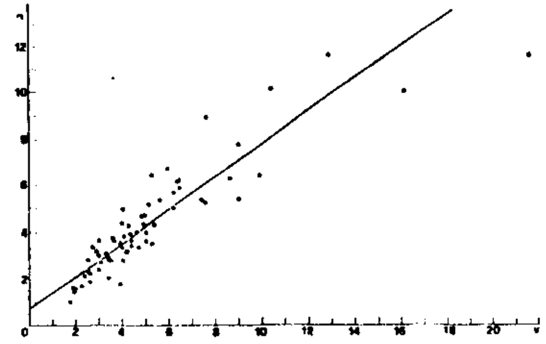

Fig. 8. Scatter diagram of n vs. $v = (p+q)/2 \simeq p \simeq q$. The correlation coefficient is $\varrho = 0.93$ and the best regression line is $n = 0.7\, v + 0.6$

Now if we fit the experimental distributions of ξ with a general β distribution

$$\beta(\xi) = \frac{\Gamma(p+q)}{\Gamma(p)\,\Gamma(q)}\, \xi^{q-1}(1-\xi)^{p-1} \qquad (8)$$

we expect a good fit with $p = q = n$ for every distribution.

Actually we have a good fit for 90% of our distributions (one example is reported in Fig. 6) and $p \simeq q \simeq n$ as we can see from the scatter diagrams of Figs. 7 and 8. In fact, from Fig. 7 we can deduce that p and q are strongly correlated ($\varrho = 0.93$) and the regression line $p = 1.0\, q + 0.7$, is compatible with $p \simeq q$. From Fig. 8 moreover, we can deduce that $\frac{(p+q)}{2} \simeq p \simeq q$ is approximately equal to n with a correlation coefficient $\varrho = 0.93$.

The variables ξ and $1 - \xi$ can be interpretated as the probabilities of perceiving the cube down and up respectively, as sampled in a single period.

The mean $\bar{\xi}$ and the variance σ_ξ^2 of the β distribution (8) are

$$\bar{\xi} = \frac{q}{p+q} \qquad \sigma_\xi^2 = \bar{\xi}\, \frac{p}{(p+q)(p+q+1)}\,. \qquad (9)$$

As we have seen $p \simeq q \simeq n$ for all subjects, hence

$$\bar{\xi} \simeq \frac{1}{2}\,, \quad \sigma_\xi^2 \simeq \frac{1}{4} \cdot \frac{1}{2n+1}\,. \qquad (10)$$

From these equations it follows that the mean probability is the same for all subjects and the perceptual behaviour of each subject can be described by the variance only.

8. Discussion

The previous results can be regarded as an attempt to explore quantitatively a field in which the very high variability seems to make unavoidable the statistical approach here described.

Without giving to the particular representation with the gamma distribution (1) any special meaning for the moment, we believe that it is worth noting that we can describe the behaviour of a subject in different perceptual situations with the same distribu-

tween the two parameters n, b suggests that the underlying neural mechanism, giving rise to the observed interval distribution is in some way "simpler" than could be expected.

We note that the first Eq. (10) $\bar{\xi} \simeq \frac{1}{2}$ shows that the perceptual entropy (Borsellino, 1967), as determined in these experiments, is $H(\xi, 1-\xi) \simeq 1$ bit. We point out that the stimulus reaching the retinae of the subjects has some well defined informational (or entropy) content $H(S_2)$, as a two dimensional optical stimulus S_2. When this stimulus is utilized as a signal for a 3-dimensional object O_3 a conditional information $H(O_3 | S_2)$, derived from the internal storage and processing, must be added to $H(S_2)$. In ordinary perceptual situations this additional information can be very small, can be practically zero as a consequence of strong correlations; the decoding of the optical signals in terms of 3-dimensional objects is therefore unambiguous.

In our case the neural machinery operates at the largest ambiguity level (1 bit) for the two possible alternatives O_3', O_3'' decoding the same optical input S_2. It is interesting to further explore if this working mode is a consequence of an inherent tendency as an expression of equal availability of the two interpretations, once the two stored conditional informations $H(O_3' | S_2)$, $H(O_3'' | S_2)$ have been retrieved. The above tendency can be looked upon as an ergodic property of the search mechanism or as an indication that the inductive process $S_2 \to O_3$ uses the principle of the entropy maximum.

The gamma distribution suggests directly a variety of possible processes. One is a threshold process, in which the threshold can be reached by the convergence at the decision region of a number of independent excitations.

By further investigations on this line, that we are continuing, we hope to get more insights and therefore to be in a better position to take some of the possible models more seriously that we are able to now.

Acknowledgements. We thank E. Gaggero and L. Trapedini for technical help in the construction of the experimental

References

Borsellino, A.: Interaction between information channels and perceptual equivocity. Atti Conv. Ann. Gruppo Naz. Cibern. CNR, April 1967, 57–60, Pisa.

Brown, K. T.: Factors affecting rate of apparent change in a dynamic ambiguous figure as a function of observation time. Wright Air Develop. Center Techn. Rep. 53-482, 1–32 (1953).

— Rate of apparent change in a dynamic ambiguous figure as a function of observation time. Amer. J. Psychol. **68**, 358–371 (1955).

— Complete interocular transfer of an adaptations process responsible for perceptual fluctuations with an ambiguous visual figure. Vision Res. **2**, 469–475 (1962).

Cohen, L.: Perception of reversible figures after brain injury. Arch. Neurol. Psych. (Chic.) **81**, 119–129 (1959).

Frederiksen, N. O., Guilford, J. P.: Personality traits and fluctuations of the outline cube. Amer. J. Psychol. **46**, 470–474 (1934).

Washburn, M. F., Mallay, H., Naylor, A.: The influence of the size of an outline cube on the fluctuation of its perspective. Amer. J. Psychol. **43**, 484–489 (1931).

Prof. A. Borsellino
Laboratorio di Cibernetica e Biofisica
I-16032 Camogli/Italia
Via Mazzini 72

Universitätsdruckerei H. Stürtz AG Würzburg
Printed in Germany

PERCEZIONE DI FIGURE AMBIGUE IN COPPIE DI GEMELLI MONOZIGOTI E DIZIGOTI

A.Borsellino (°), S.Rinesi (°°)

I primi risultati ottenuti sullo studio del fenomeno di inversione di figure ambigue hanno messo in luce una riproducibilità del comportamento dei soggetti di fronte a questi patterns e una stretta correlazione fra i parametri n-b che definiscono la curva di distribuzione dei tempi di inversione, ben rappresentata dalla Gamma di Eulero [1]

$$\Gamma(t) = \frac{(bt)^n e^{-bt}}{t\,\Gamma(n)} \qquad (1)$$

Questo ha suggerito di sottoporre il test dei patterns ambigui a coppie di gemelli monozigoti (MZ), cioé identici, e dizigoti (DZ), cioè diversi, cercando di determinare un'eventuale influenza di un fattore genetico. A questo scopo si sono esaminate 16 coppie di gemelli MZ e 16 coppie di gemelli DZ, di condizioni socioeconomiche equivalenti, ottenendo così che l'unico parametro diverso fosse lo zigotismo . La diagnosi di zigotismo era basata quasi per tutti i casi sui gruppi sanguigni, con una probabilità di solo il 5% che i gemelli dizigoti avessero gli stessi 5 gruppi sanguigni.

(°) Lab.Cib.Biofis. CAMOGLI
(°°) Ist. Fisica GENOVA

Cybernetic Congr. 1971, Ital Soc. for Cybern. and Biophysics
Casciana Terme

L'età era compresa tra i 16 e i 20 anni, e nessuno dei soggetti esaminati conosceva il fenomeno dei patterns ambigui. I dati sono stati registrati dopo alcuni minuti di training. Per vedere se questo campione aveva lo stesso comportamento dei soggetti precedentemente esaminati 1 sono state fatte prove di riproducibilità ed è stata calcolata la correlazione tra i parametri n-b che definiscono la curva di distribuzione Gamma di Eulero (1), che ha fornito risultati positivi; cioè anche i dati relativi a questo gruppo di soggetti sono riproducibili, e la correlazione n-b ha il valore $\rho_{n-b} = 0.86$.

E' stata quindi calcolata la correlazione fra i parametri n_1-n_2, b_1-b_2, t_1-t_2 (tempi medi di inversione) dove gli indici 1 e 2 si riferiscono agli elementi di ogni coppia, mediante la correlazione intraclasse [2] , definita da

$$\rho = \frac{K\sigma_m^2 - \sigma^2}{(K-1)\,\sigma^2}$$

dove K = 2 elementi della classe (2 gemelli)

σ_m^2 = varianza delle medie calcolate su ogni coppia

σ^2 = varianza complessiva

Si è impiegato questo metodo poiché si tratta di due risposte allo stesso stimolo ed è pertanto necessario tenere conto delle combinazioni che si possono formare all'interno degli elementi che compongono la coppia.

Per la significatività di questa corelazione si trasforma il coefficiente di correlazione trovato in z di Fischer, si aggiunge un fattore correttivo ottenendo z corretto, che si confronta con l'errore $\varepsilon_{z_c} = \frac{1}{N-\frac{3}{2}}$ in cui N è il numero dei soggetti esaminati. La probabilità che il valore trovato non sia casuale è $P<0.05$ se

$z_c > 1.96\,\varepsilon_{zc}$

I risultati ottenuti forniscono dei valori di correlazione significativi per i gemelli monozigoti e non significativi per i dizigoti, come appare dalla seguente tabella

MZ	DZ
$\rho_{n_1-n_2} = 0.46$	$\rho_{n_1-n_2} = 0.05$
$\rho_{b_1-b_2} = 0.76$	$\rho_{b_1-b_2} = 0.35$
$\rho_{t_1-t_2} = 0.79$	$\rho_{t_1-t_2} = 0.11$
$P < 0.05$	non significativo

e come viene ben visualizzato nelle figg. 1 e 2.

E' quindi ben evidente una componente genetica significativa che si aggiunge agli altri dati già ottenuti allo scopo di cercare un modello che ben rappresenti questo fenomeno; questi risultati stimolano anche ad approfondire l'esame del fattore genetico con un confronto fra fratelli gemelli e un loro sibling, cioè un fratello non gemello.

— — — —

Si ringrazia il prof. Gedda, Direttore dell'Istituto di Genetica e Gemellologia G.Mendel, che con la sua collaborazione ha permesso lo svolgimento di questo lavoro.

[1] A.Borsellino, A. De Marco, A. Allazetta, S. Rinesi, B.Bartolini - Distribuzione dei tempi di inversione nella percezione di figure ambigue. Congresso di Cibernetica - Casciana Terme (PISA) 11-13 ottobre 1971.

[2] Degrada, Ercolani, Saggesi - Riv. Psic. 1966,60,135

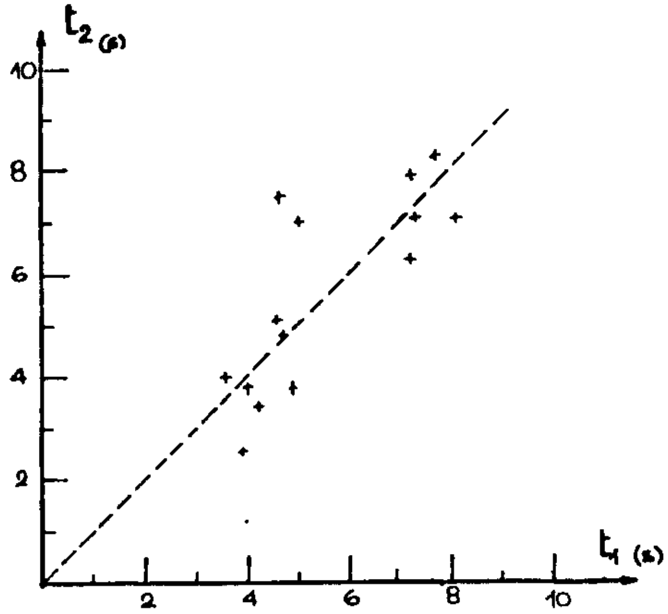

FIG 1 Distribuzione dei tempi medi di inversione rispetto alla retta a 45°. Gemelli monozigoti

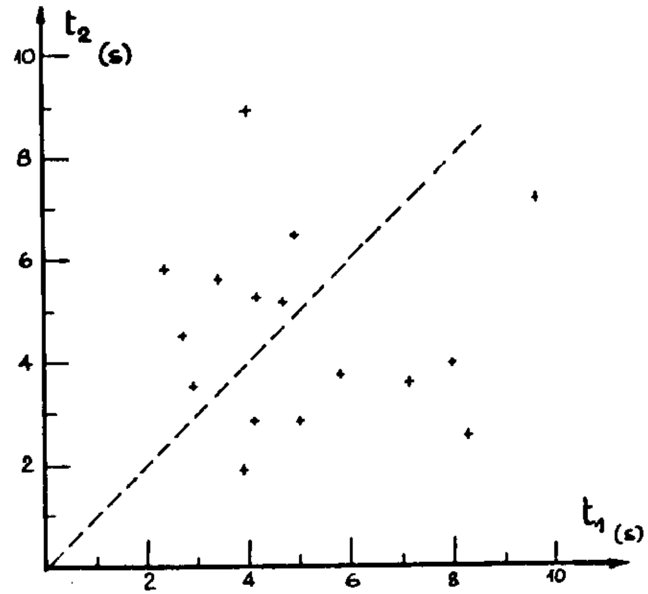

FIG. 2 Distribuzione dei tempi medi di inversione rispetto alla retta a 45°. Gemelli dizigoti

Biol. Cybern. 55, 377–385 (1987)

Biological Cybernetics

Statistical Properties of Flip-Flop Processes Associated to the Chaotic Behavior of Systems with Strange Attractors

F. Aicardi[1] and A. Borsellino[1,2]

[1] ISAS – International School for Advanced Studies, I-34014 Trieste, Italy
[2] ICTP – International Center for Theoretical Physics, I-34014 Trieste, Italy

Abstract. The chaotic behavior of systems with strange attractors can be discussed by examining the flip-flop process associated to the system dynamics. This was already shown by Lorenz (1963) in his first seminal paper. A somewhat surprising result was obtained by Aizawa (1982), who, studying the same Lorenz attractor at the parameter value $r=28$, reached the conclusion that the associated flip-flop was a typical Markov process. Since the process is generated in a deterministic way, one may wonder if the Aizawa result is accidental, depending on the particular parameter value, or if a similar conclusion can be extended to other systems, with different attractors. Our conclusions are that the Aizawa result is mostly accidental, because for other parameter values and for other attractors there are sharp deviations from the Markovian process.

1 Introduction

In our search for neuronal modeling of transitions between two alternative perceptual states in continuous observation of ambiguous patterns (Necker cube, etc.), we found difficult to explain the long time scale of the process and the stochastic character of the transitions (Borsellino et al. 1972). A way out could be to attribute to the neuronal system the possibility to enter a stochastic regime dominated by a strange attractor with at least two basins of attraction.

For this reasons we were motivated to study the statistical properties of the flip-flop process associated with a strange attractor. In particular we were interested to verify in which cases a markovian characteristic can be recognized and/or demonstrated.

2 The Flip-Flop Process: Statistical Analysis

For systems with two attracting basins, as for the Lorenz or for the Rikitake (Cook and Roberts 1970) system, the flip-flop process is identified by the passage of the trajectory point from one basin to the other, after a more or less lengthy time of permanence in them. For the Roessler (1976) attractor, with one basin only, the two states can be defined by the two opposite faces of the "Moebius" ribbon on which the trajectories unroll, alternating from one face to the other (see Figs. 1–3).

Calling L and R the system states corresponding to the positioning of the trajectory point in the left or the right basin for the Lorenz or Rikitake systems (we could call U and D the two up and down states in the Roessler case), the system dynamics will generate a sequence of states as RLRRL..., the states being observed after each turn of the trajectory.

Calling $p(\mathrm{L})$, $p(\mathrm{R})$ the probabilities of finding the system in the L or R state, the system symmetry between L and R states, gives $p(\mathrm{L})=p(\mathrm{R})=1/2$. The transition probabilities $p(\mathrm{L}|\mathrm{L})$, $p(\mathrm{R}|\mathrm{L})$, ..., in the case of a Markov chain of events should come out to be independent of time.

Calling P the jump probability, for the same system symmetry we have $P=p(\mathrm{L}|\mathrm{R})=p(\mathrm{R}|\mathrm{L})$ while for the permanence probability $p(\mathrm{L}|\mathrm{L})=p(\mathrm{R}|\mathrm{R})=1-P$.

For a chain like RLRRRLRLL ... the corresponding chain YYNNYYYN ..., where Y stays for "jump occurrence" and N for "no jump occurrence", if the chain of events is Markovian, allows us to obtain the probability that the trajectory point, after entering a basin (the entering jump), will execute there m turns before leaving it with another jump (the exit jump) $p(m)=P(1-P)^{m-1}$. In the same manner the probability to observe J jumps after M turns is given by:

$$p(J|M)=\binom{M}{J}P^{J}(1-P)^{M-J}. \tag{2.1}$$

These probabilities can be estimated from chains long enough to be considered as representative statis-

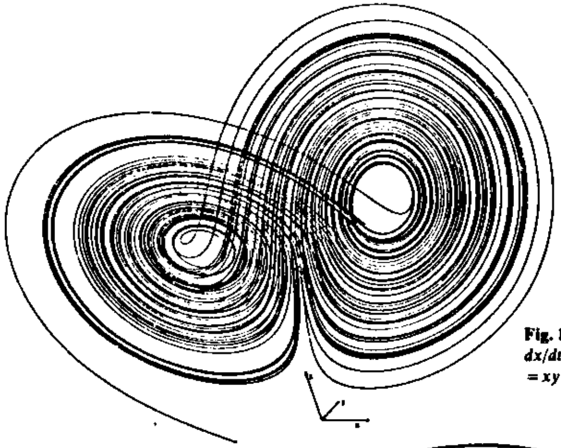

Fig. 1. The Lorenz attractor at $r=50$ ($b=8/3$): $dx/dt=-10x+10y$; $dy/dt=-xz+rx-y$; $dz/dt=xy-bz$

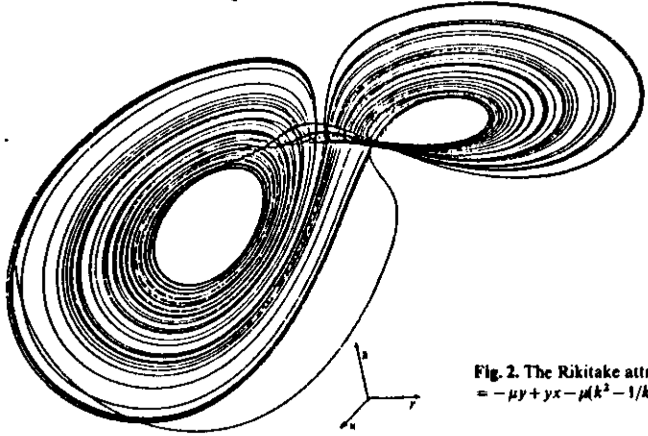

Fig. 2. The Rikitake attractor at $\mu=1$, $k=2$: $dx/dt=-\mu x+yz$; $dy/dt=-\mu y+yx-\mu(k^2-1/k^2)x$; $dz/dt=1-xy$

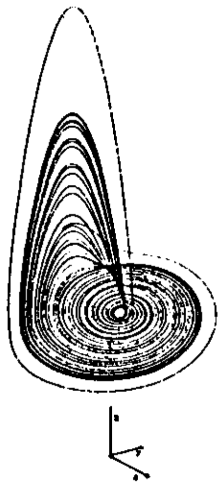

Fig. 3. The Roessler attractor at $r=0.2$, $s=8.7$: $dx/dt=-y-z$; $dy/dt=x+ry$; $dz/dt=r+z(x-s)$

tical samples, using:

$$p(m)=1/N\sum_{k=1}^{N}\delta_{m,i_k}, \tag{2.2}$$

where $\delta_{m,l}$ is the usual Kroneker symbol; $i_1, i_2, \ldots, i_N$ represent the number of turns executed in a basin after a jump; N is the number of jumps in the sample. Similarly:

$$p(J|M)=1/T\sum_{k=1}^{T}\widehat{\delta J, J_k}. \tag{2.3}$$

$J_1, J_2, \ldots, J_T$ being the number of jumps occurring in each of the T sequencies of M turns in which the total sample is subdivided.

In Figs. 4–6 we show (crosses) the results obtained for the Lorenz equations with $r=50$ and for the Rikitake and Roessler attractors. The solid lines give the expected distributions, computed from (2.1) with

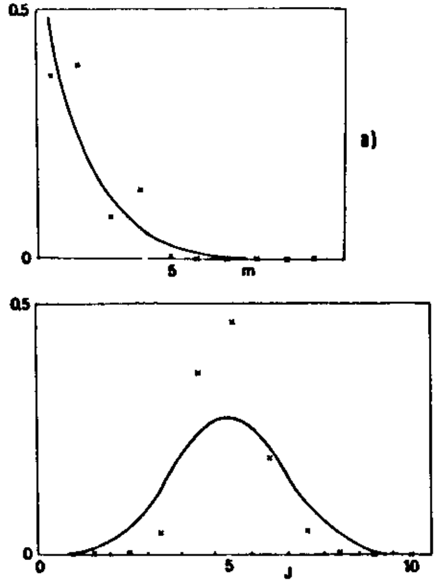

Fig. 4a, b. The $p(m)$ and the $p(J|M)$ ($M=10$) for the Lorenz attractor at $r=50$. The corresponding P value is 0.5132

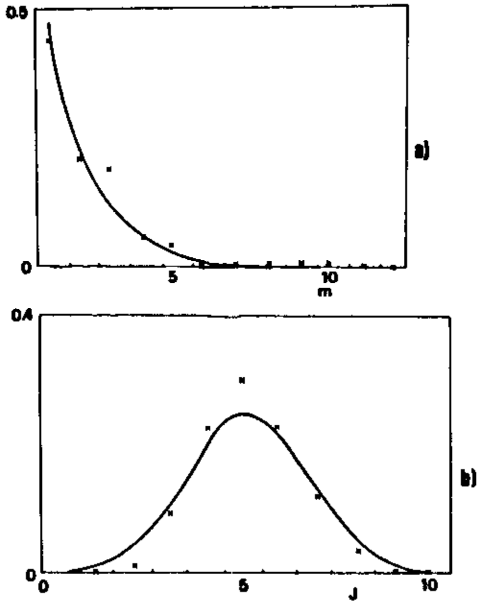

Fig. 5a, b. The $p(m)$ and the $p(J|M)$ ($M=10$) for the Rikitake attractor at $\mu=1$, $k=2$. The corresponding P value is 0.3231

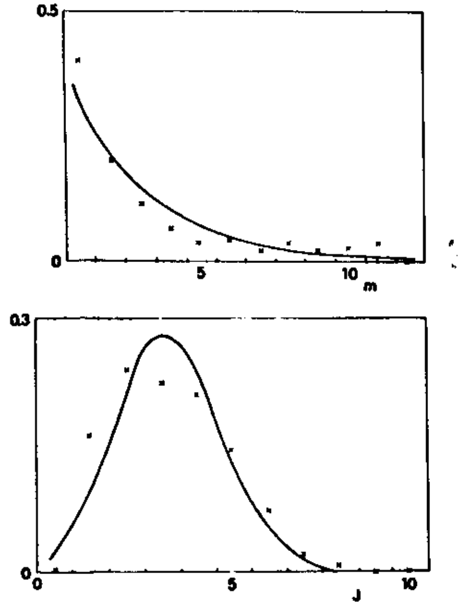

Fig. 6a, b. The $p(m)$ and the $p(J|M)$ ($M=10$) for the Ro
attractor at $r=0.2$ and $s=8.7$. The corresponding P value is

the P value estimated from the total sample. The
not satisfactory, showing, at variance with the Aiz
conclusion, that the flip-flop process is not a r
Markovian one. In the next paragraph we discu
possible way to examine the nature of the ch
process and how far it can approach a Marko
process.

3 The Monodimensional Maps

When studying strange attractors, in particular
stability of their periodic orbits, certain monodi
sional maps were found useful (Shaw 1981).

They are obtained numerically (by computer) i
following way: the maximum value reached l
selected dependent quantity in a turn inside the ba
placed versus the maximum reached in the follo
turn. Thus graphics of functions arise (that is not
trivial). They have the common characteristic of loo
continuous and monotonic on two intervals, so defi
a "one at two" correspondence (Figs. 7, 8, an
Moreover, changing a system parameter, a fami
functions is generated.

The maps, starting from a generic initial v
generate a succession of values correspondin

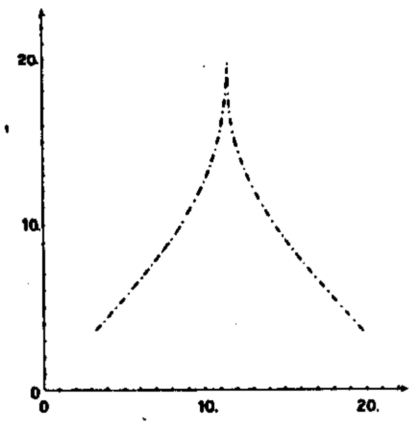

ɪ. 7. The monodimensional map associated with the Lorenz ractor at $r=28$. M_n is the maximum of y in the n-th turn

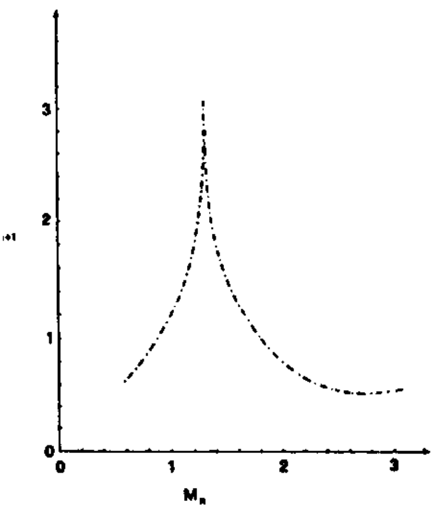

ig. 8. The monodimensional map associated with the Rikitake ttractor at $\mu=1$ and $k=2$. M_n is the maximum of z in the n-th ırn

ubsequent maximum values of the selected quantity at very turn. It may occur that at certain parameter alues the map iterations converge to one point, or to a et of n periodic points. Clearly these points correspond with subsequent maximum values recurring eriodically, and hence indicate that the solution is a ı-periodic orbit (the period being the duration of a turn n a basin).

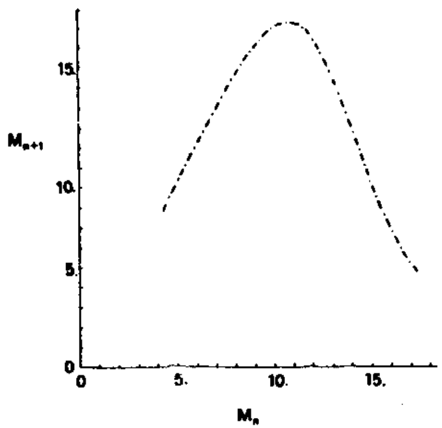

Fig. 9. The monodimensional map associated with the Roessler attractor at $r=0.2$ and $s=8.7$. M_n is the maximum of x in the n-th turn

It can be shown that the above fact occurs to families of maps of this type for an infinite but enumerable set of parameter values (Collett-Eckmann 1980); for all the other values the solutions are not periodic and hence they are of interest in studying chaotic processes. This is our case.

The succession of values (one for each turn), obtained from the iterated map, does not describe the chaotic process of basin change. In fact the chosen variable quantity, due to the symmetry between the two basins, shows an exactly alike behaviour in the two basins.

A more careful examination of the maximum values successions and of the corresponding chains of left and right (or up and down) states, allowed us to find that the map, given the value M_n of the maximum in the n-th turn, can tell both the following value M_{n+1} and whether the $(n+1)$-th turn will be in the same basin as the n-th or not.

In fact, calling M_c the abscissa of the absolute maximum of the map, one has: if $M_n < M_c$, the $(n+1)$-th turn will be in the same basin as the n-th; if $M_n > M_c$, will be in the opposite one.

Then by the map iteration one can generate, with the succession of infinite different values, also a two-value random process. Thus we are lead to analyse a two-valued random chain generated by iterated functions on $(0,1)$, similar to the maps obtained from the temporal evolution of system with strange attractors. The advantage of this substitution lies in the possibility of replacing about one thousand steps of Runge-Kutta (fourth order) integration by the simple iteration of the

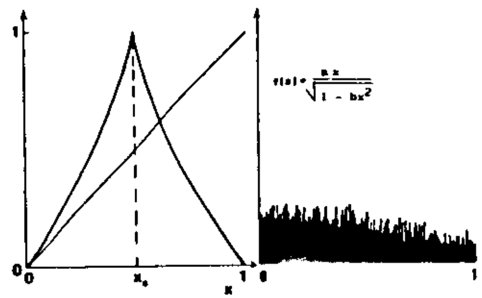

Fig. 10. A function of family $F_1 (b=2)$ and its $q(\Delta x_i)$. The value of a is such that $f(x_c)=1$

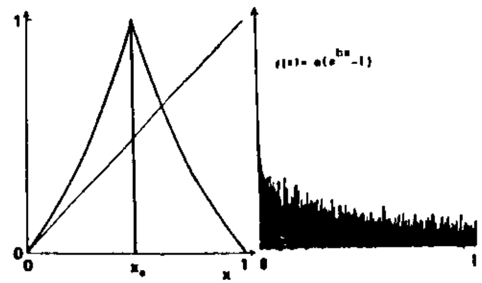

Fig. 11. A function of family $F_2 (b=1.8)$ and its $q(\Delta x_i)$. The value of a is such that $f(x_c)=1$

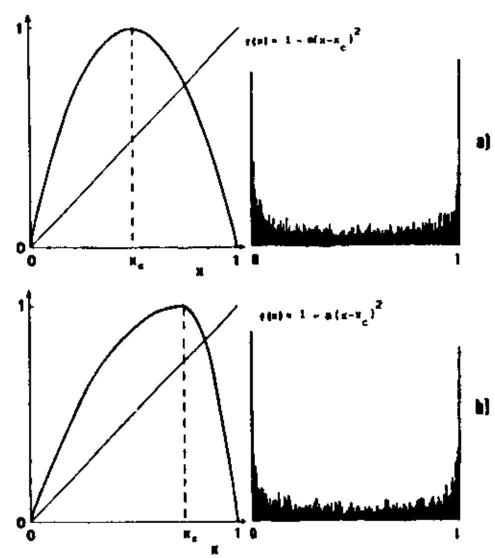

Fig. 12a, b. Two functions of family F_3 (with $x_c=0.5$ and $x_c=0.75$) and their $q(\Delta x_i)$. The values of a are such that $f(0)=f(1)=0$

map. We take at least five thousand values, one for every turn, to form the chain we analyze.

The tested maps are shown in Figs. 10–12; the corresponding families are called F_1, F_2, F_3. These generate processes qualitatively similar to those obtained from strange attractors. The results of the statistical analysis of the two-value chains generated from them are shown in Figs. 13–15. The map families F_1 and F_2 tend, for particular values of parameters, to a linear map which, on numerical examination, gen-

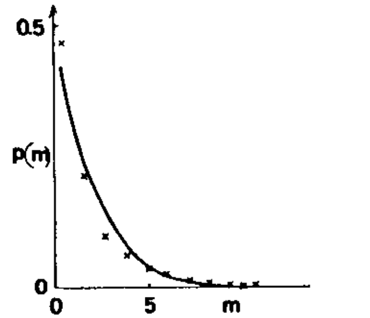

Fig. 13. The $p(m)$ for the map of F_1 with $b=1.8$

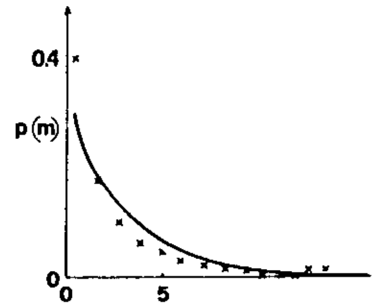

Fig. 14. The $p(m)$ for the map of F_2 with $b=1.95$

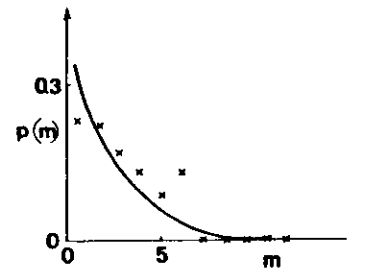

Fig. 15. The $p(m)$ for the map of F_3 with $x_c=0.85$

erates a Markovian process with $P=0.5$. The same happens for the map of the F_3 family, with the x_c value equal to 0.5 (see Fig. 12a).

4 Markovian Maps

We call Markovian a map able to generate, by the method of Sect. 2, Markovian chains. If a Markovian map exists for each P value, the analogies of the attractor chaos with Markovian chaos would be assessed by the likeness between its associated map and the Markovian one. We will show how we found two families of Markovian maps.

It is useful to consider that for the functions of F_1 and F_2, which are symmetric (about the middle point 0.5), the P value decreases while the cusp becomes narrow, and for the family F_3, asymmetrical, P decreases while the x_c value increases.

Now we recall what the P value means for the generic map in the considered process: it indicates the probability for the generic iteration of finding a value greater than x_c, the abscissa of maximum. To estimate the value of P it is necessary to know the probability distribution associated with the map $f(x)$ and defined as follows:

$$q(x)=\lim_{N\to\infty} 1/N \sum_{n=1}^{N} \delta\{x-f^n(x_0)\}, \tag{4.1}$$

where x_0 is a generic point of the interval (0, 1) and f^n is the n-th iteration of f on x_0. In our case an approximate $q(x)$ related to the maps is obtained from computer by the following estimate:

$$q(\Delta x_i)=1/N \sum_{n=1}^{N} \delta_{i,j_n}, \tag{4.2}$$

where $q(\Delta x_i)$ is the normalized frequency for $f^n(x_0)$ ending in the i-th interval Δx_i, obtained by the partitioning of (0, 1). In Figs. 10–12 the $f(x)$ are shown together with their $q(\Delta x_i)$. Let us recall that the P value can now be computed for the map by:

$$P=\lim_{N\to\infty} 1/N \sum_{n=1}^{N} h(n)\begin{cases} h(n)=1 & \text{if } f(x_0)>x_c \\ h(n)=0 & \text{if } f(x_0)\leq x_c . \end{cases} \tag{4.3}$$

The (4.3) is equivalent to

$$P=\int_{x_c}^{1} q(x)dx. \tag{4.4}$$

The $p(m)$ values are computed from the map iteration as follows:

$$p(m)=\lim_{N\to\infty} 1/N \sum_{n=1}^{N} h(n)\bar{h}(n+1)$$
$$\times \bar{h}(n+2)\ldots\bar{h}(n+m-1)h(n+m), \tag{4.5}$$

where $h(n)$ is the same as in (4.3) and $\bar{h}(n)=1-h(n)$.

We search again for the locus of points of (0, 1) mapped into the subset $(x_c, 1)$ after m (and not less) map iterations. These subsets may be characterized as follows:

$$I_m=f^{-m}(x_c,1)\backslash\left[f^{-m}(x_c,1)\cap\left\{\bigcup_{k=0}^{m-1} f^{-k}(x_c,1)\right\}\right], \tag{4.6}$$

where $f^0(a,b)$ is by definition the same (a,b). It results that $I_0=f^0(x_c,1)=(x_c,1)$. The Fig. 16 shows the I_m ($m=1,\ldots,4$) for a generic map. Now we have:

$$p(m)=\int_{I_{m-1}} q(x)dx \tag{4.7}$$

and

$$p(1)=\int_{I_0} q(x)dx=\int_{x_c}^{1} q(x)dx=P$$

corresponding to (2.2).

The conditions that must be satisfied for the process to be Markovian are expressed by the infinite set of equations:

$$\int_{I_{m-1}} q(x)dx=P(1-P)^{m-1} \quad (m=1,\ldots,\infty), \tag{4.8}$$

where

$$P=\int_{x_c}^{1} q(x)dx.$$

We can call Markovian the function satisfying these conditions. From the shape of the $q(x)$ relative to the maps of F_1, F_2, and F_3, one can observe that these conditions will not be generally satisfied. To find them

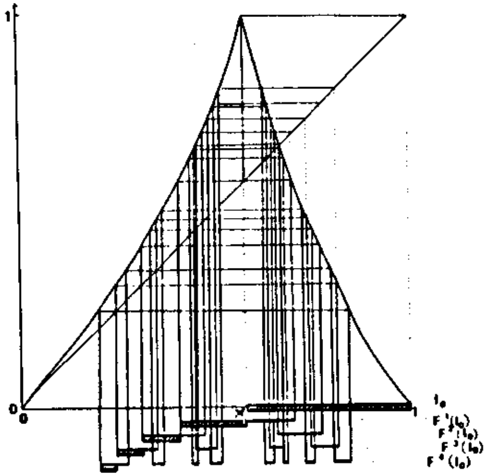

Fig. 16. The intervals I_m (see text) are dashed

in the case of a Markovian chain, we consider the map M_0:

$$y=2x \quad \text{for} \quad x<0.5,$$
$$y=2(1-x) \quad \text{for} \quad x>0.5.$$

Its probability distribution $q(x)$ is constant. From the normalization on (0, 1), we obtain $q(x)=1$. In this simple case the (4.7) is reduced to

$$p(m)=L(I_{m-1}), \tag{4.9}$$

where $L(I)$ is the measure of the interval I.

The generic interval I_k is mapped by M_0 on an interval I_{k+1} of double length. It follows, being $L(I_k)=L(I_{k-1})/2$:

$$p(1)=L(I_0)=0.5$$
$$p(2)=L(I_1)=0.5/2 \tag{4.10}$$
$$\ldots\ldots$$
$$p(m)=L(I_{m-1})=0.5/2^{m-1}.$$

The (4.10) may be interpreted as $p(m)=P(P-1)^{m-1}$, being $P=(1-P)=0.5$ and the (4.8) is satisfied.

We now wish to find maps able to generate Markovian flip-flop processes without symmetry between the two transition events. The symmetry in the case of M_0 follows from the symmetry of $f(x)$ and its distribution $q(x)$ about $x=0.5$. To obtain a P value different from 0.5, it is enough to give up only one of these symmetry conditions. Indeed we obtain a family of Markovian maps asymmetrical but with $q(x)$ symmetrical (called M_1), and another family (called M_2) of symmetrical functions with $q(x)$ asymmetrical. At $P=0.5$ both M_1 and M_2 maps are identical to M_0.

They are:

M_1 (see Fig. 17)

$$y=ax \quad \text{for} \quad x<x_c$$
$$y=a(1-x) \quad \text{for} \quad x>x_c$$

where $a=1/x_c$, a varying from 1 to infinity. Their $q(x)$ are still equal to 1 in (0, 1); being $L(I_k)=L(I_{k-1})/a$, it

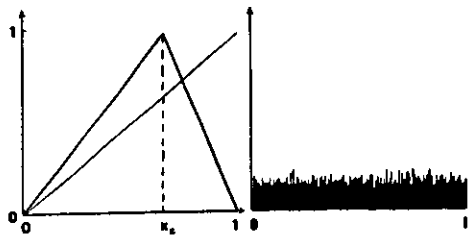

Fig. 17. The map of family M_1 with $a=1.5$ and its $q(\Delta x_i)$

follows:

$$P=p(1)=L(I_0)=1-x_c=(a-1)/a$$
$$p(2)=L(I_1)=(1/a)(a-1)/a \tag{4.1}$$
$$\ldots\ldots$$
$$p(m)=L(I_{m-1})=(1/a)^{m-1}(a-1)/a.$$

The (4.11) coincide exactly with (4.8), bei $P=(a-1)/a$ and $1-P=1/a$.

M_2 (see Fig. 19a and b):

$$y=ax \quad \text{for } 0<x<1/2a$$
$$y=ax/(a-1)+1-a/2(a-1) \quad \text{for } 1/2a<x<1/2$$
$$y=-ax/(a-1)+1-a/2(a-1) \quad \text{for } 1/2<x<1-1$$
$$y=a(1-x) \quad \text{for } 1-1/2a<x<$$

Their probability distributions are constant on two intervals (0, 1/2) and (1/2, 1) (see Fig. 18a and

By the normalization in (0, 1) $q(x)$ results:

$$q(x)=2/a \quad \text{for} \quad x<1/2,$$
$$q(x)=2(a-1)/a \quad \text{for} \quad x>1/2. \tag{4.}$$

Thus

$$P=\int_{1/2}^{1} q(x)dx=\int_{1/2}^{1} 2(a-1)/a\, dx=(a-1)/a.$$

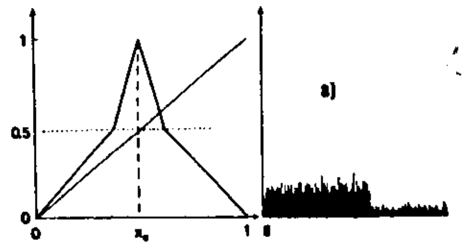

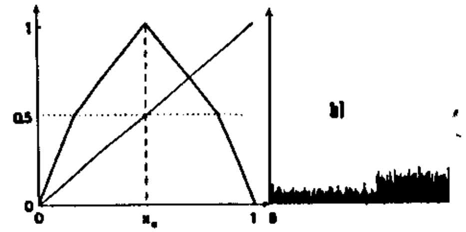

Fig. 18a, b. The maps of family M_2 and their $q(\Delta x_i)$ wi $a=1.3$; b $a=3$

Since the (4.7) may be written in this case

$$m) = L(I_{m-1})q(I_{m-1}),$$

here $q(I_k)$ is the value of $q(x)$ in the I_k interval, and iving $L(I_0) = 1/2$, $L(I_1) = (a-1)/2a$, $L(I_k) = L(I_{k-1})/a$ $\geqq 2$), and $q(I_0) = 2\ (a-1)/a$, $q(I_k) = 2/a$ $(k \geqq 1)$, we ill obtain, in agreement with (4.8):

$$m) = (1/a)^{m-1}(a-1)/a = P(1-P)^{m-1}.$$

Besides the families M_1 and M_2 we analized on the mputer the chaotic chains generated from other nctions continuous and linear on subsets of (0, 1). We ver obtain Markov chains. The dissimilarity beeen the Markovian maps and the maps related to the range attractors makes us able to tell how the aotic process of a strange attractor diverges from a larkov chaos. Even in generalizing the simple Marv processes to the Markov processes with finite emory one can show, with similar but tedious guments, that the maps related to the strange tractors are generally unable to generate processes of is type.

Entropy for the Strange Attractors

he apparent Markovian character of the Lorenz aos lead Aizawa to evaluate the Kolmogorov-Sinai tropy H_{KS} and the Hausdorff dimension D_H via the p-flop process:

$$_{KS} = -\{P_{++} \ln P_{++} + P_{+-} \ln P_{+-}\}, \tag{5.1}$$

$$)_H = H_{KS}/\ln 2. \tag{5.2}$$

From $P_{+-} = P_{-+} = P = 0.44$ and $P_{++} = P_{--}$ $(1-P) = 0.56$, for the chaos of the Lorenz tractor at $r = 28$, one obtains $H_{KS} = 0.686$ and $_H = 0.989$.

This simplified estimate is in good agreement with ther estimates (Collett-Eckmann). We observe that e simplified procedure cannot be used when the atistical process is non-Markovian.

To obtain an estimate for non-Markovian prosses, we notice that

$$_H = -\{(1-P)\lg_2(1-P) + P\lg_2 P\}$$

presents the Lyapunov number N_L computed for oth the Markovian maps of M_1 and M_2 (with the aracteristic value P). In fact for M_1 one obtains:

$$
\begin{aligned}
{}_L &= \int_0^1 q(x)\lg_2\{|df(x)/dx|\}dx \\
&= \int_0^{1-P} \lg_2\{a\}dx + \int_{1-P}^1 \lg_2\{a/(a-1)\}dx \\
&= (1-P)\lg_2\{1/(1-P)\} + P\lg_2\{1/(1-P)\} = D_H
\end{aligned}
\tag{5.3}
$$

while for M_2

$$
\begin{aligned}
N_L = & \int_0^{(1-P)/2} (1-P)\lg_2\{1/(1-P)\}dx \\
& + \int_{(1-P)/2}^{1/2} (1-P)\lg_2\{1/P\}\,dx \\
& + \int_{1/2}^{1-(1-P)/2} P\lg_2\{1/P\}\,dx \\
& + \int_{1-(1-P)/2}^{1} P\lg_2\{1/(1-P)\}\,dx \\
= & (1-P)\lg_2\{1/(1-P)\} + P\lg_2\{1/P\} = D_H.
\end{aligned}
$$

This relation between Hausdorff dimension and Lyapunov number may be extended to non-Markovian maps. For a strange attractor the entropy can be obtained from the Hausdorff dimension, that is from the Lyapunov number, of its monodimensional map.

The idea of attributing an entropy to the disorder generated from map iterations has been already discussed (Shimada 1979). When the entropy is proportional to the Lyapunov number, it could assume also negative values. This fact is interpretable as the property of the map of generating order instead of chaos. The negative value of the Lyapunov number is indeed characteristic of functions whose iterations converge to stable periodic cycles (Ott 1981).

A final observation can be made when comparing the Hausdorff dimension to the Lyapunov number: the function $f(x) = 4x(1-x)$ that results (experimentally) Markovian with $P = 0.5$ (see Sect. 2), has the Lyapunov number $N_L = 1$. (For this function we know the analytic expression of the probability distribution $q(x) = 1/\{\pi\sqrt{[x(1-x)]}\}$.) It is exactly the Lyapunov number of the map M_0 (see Sect. 3) generating Markov chains with $P \approx 1/2$. This fact suggests another conjecture: two maps, that generate the same Markov chaos, must have the same Lyapunov number. That should be a necessary condition only. It seems satisfied for all the Markovian maps which we have analyzed.

Acknowledgement. The AA thank S. Stabile (SISSA) for the expert assistance and help in the graphical part of the work.

References

Aizawa Y (1982) Global aspects of the dissipative dynamical systems. Prog Theor Phys 68:64–84

Borsellino A, DeMarco A, Allazetta A, Rinesi S, Bartolini B (1972) Reversal time distribution in the perception of visual ambiguous stimuli. Kybernetik 10:139–144

Collett P, Eckmann JP (1980) Iterated maps on the unit interval as dynamical systems. Birkhäuser, Boston

Cook AE, Roberts PH (1970) The Rikitake two-disc dynamo system. Cambridge Philos Soc 78:547–569

Lorenz E (1963) Deterministic nonperiodic flow. J Atmos Sci 20:130–141

Ott E (1981) Strange attractors and chaotic motions of dynamical systems. Rev Mod Phys 53:655–671

Roessler OE (1976) An equation for continuous chaos. Phys Lett A 57:397–399

Shaw R (1981) Strange attractors, chaotic behaviour, and information flow. Z. Naturforsch A 36:80–112

Shimada Y (1979) Gibbsian distribution on the Lorenz attractor. Prog Theor Phys 62:61–69

Received: August 4, 1986

Prof. Dr. A. Borsellino
ICTP International Center for
Theoretical Physics
Strada Costiera 11
I-34014 Trieste
Italy